Unbound Spinons in the $S=1/2$ Antiferromagnetic Chain $KCuF_3$

D. A. Tennant, T. G. Perring,[a] and R. A. Cowley
Department of Physics, Clarendon Laboratory, University of Oxford, Parks Road, Oxford, United Kingdom

S. E. Nagler
Department of Physics, University of Florida, Gainesville, Florida 32605
(Received 8 February 1993)

Inelastic neutron scattering has been used to study the temperature dependence of the magnetic response in the one-dimensional $S=1/2$ Heisenberg antiferromagnet $KCuF_3$. The scattering is consistent with that expected for unbound spinon pair excitations.

PACS numbers: 75.10.Jm, 75.30.Ds, 75.50.Ee

Over the past decade there has been great interest in the ground state properties of interacting many body quantum systems, for example, high T_c superconductors [1], fractional quantum Hall states [2], and integer spin chain or "Haldane" systems [3,4]. Quantum field theory has provided a general theoretical approach to problems of this type [5]. One of the insights that has been obtained is that the fundamental excitations in these systems generally have fermion character [6–9] as opposed to the usual picture of boson excitations out of a long range ordered ground state [10]. The consequences of this idea have been most evident for Heisenberg antiferromagnetic chains (HAFC), defined by the Hamiltonian

$$\hat{\mathcal{H}}=2J\sum_r \mathbf{S}_r\cdot\mathbf{S}_{r+1}. \quad (1)$$

The underlying excitations (now called "spinons") [11] occur only in pairs [12]. It is now understood, as a consequence of the topological term in the field theoretic formulation of the problem [3], that if the spin quantum number is an integer, the spinons are bound. This leads to well defined, spin-wave-like modes exhibiting a Haldane gap. Haldane systems have been investigated extensively, both theoretically and experimentally [4,13], during recent years.

Conversely, there has been little recent experimental work on the half-odd-integer spin chains, in which the spinons are effectively free. This is in spite of the fact that the presence of unbound spinons has a strong effect on experimentally measurable quantities such as the dynamical correlation functions measured by neutron scattering. In this Letter we present the results of an inelastic neutron scattering study of the model $S=1/2$ HAFC compound $KCuF_3$. Our experimental results are incompatible with classical theory for 1D antiferromagnets [14] but can be quantitatively explained by field theory calculations for the dynamical correlation function $S^{aa}(Q,\omega)$ [15], confirming the importance of unbound spinons in this system. In particular, the neutron scattering shows a quantum continuum of excited states, and changes with temperature and wave vector as predicted by field theory.

The ground state of the $S=1/2$ HAFC can be solved exactly by the Bethe ansatz method [16]. It is a singlet with total spin $S_T=0$. des Cloiseaux and Pearson (dCP) extended this method to the calculation of the low lying excited states [17], which they interpreted as spin-wave-like states with $S_T=1$. The dCP states obey a dispersion relation

$$\epsilon_Q=\pi J|\sin(Q)|. \quad (2)$$

Unfortunately the Bethe ansatz method is not amenable to the calculation of matrix elements, so dCP could not obtain an expression for $S^{aa}(Q,\omega)$. Early neutron scattering experiments on the $S=1/2$ HAFC materials CPC [18,19] and $KCuF_3$ [20,21] were interpreted as confirmation of the dCP spectrum. Interestingly, the line broadening observed in the CPC measurements could not be explained by a simple pole in $S^{aa}(Q,\omega)$.

It was later shown by Faddeev and Takhtajan (FT) [12] that the natural excitations (spinons) actually have $S_T=1/2$, and hence are fermions. The spinons obey a dispersion relation identical to that of the dCP states [Eq. (2)]. The dCP states are now understood to be a superposition of two spinons, one of which carries zero momentum. At each Q a continuum of spinon pair states extended in energy results, the upper bound of which corresponds to two spinons each of wave vector $Q/2$,

$$\epsilon_Q^u=2\pi J|\sin(Q/2)|. \quad (3)$$

Guided by the finite chain calculations, exact results, and sum rules, Müller *et al.* (*M*) [22] constructed an ansatz for $S^{aa}(Q,\omega)$ at $T=0$ with a square-root singularity at the lower bound ϵ_Q extending to a sharp cutoff at ϵ_Q^u.

In the long wavelength, low energy limit the HAFC Hamiltonian can be mapped onto a relativistic quantum field theory. Schulz [15] exploited this mapping and the bosonization method of Luther and Peschel [23] to calculate $S^{aa}(Q,\omega)$ analytically. For integer HAFCs he found that $S^{aa}(Q,\omega)$ has a single mode with a gap as predicted by Haldane [3]. The corresponding expression for half integer HAFCs, valid near $Q=\pi$, is

0031-9007/93/70(25)/4003(4)$06.00

$$S^{aa}(Q,\omega)=(n_\omega+1)\mathrm{Im}\left[\frac{1}{T}\rho\left(\frac{\omega-vq}{4\pi k_B T}\right)\rho\left(\frac{\omega+vq}{4\pi k_B T}\right)\right], \quad (4)$$

where

$$\rho(x)=\frac{\Gamma(\frac{1}{4}-ix)}{\Gamma(\frac{3}{4}-ix)}, \quad q=Q-\pi, \quad v=\pi J.$$

Here n_ω is the Bose factor and Γ is the gamma function. In the limit of $T=0$ this yields $S^{aa}(Q,\omega)=1/[\omega^2-(vq)^2]^{1/2}$, which is the low energy limit of the form of M.

Our previous work on $KCuF_3$ [24] confirmed the existence of a continuum of excited states with bounds given by ϵ_Q and ϵ_Q^u. At low temperatures the observed neutron scattering could be satisfactorily accounted for by a square root singularity. Improvements in the experimental technique [25] have allowed us to make careful quantitative measurements as a function of temperature. As shown below, the results are in quantitative accord with the predicted spinon pair correlations in the region of validity of Eq. (4). This provides strong evidence that the field theoretic approach successfully describes the physics of the $S=1/2$ HAFC, which is manifestly a lattice system.

The single crystal of $KCuF_3$ was the same one used previously [21,24]. $KCuF_3$ has a tetragonal structure with room temperature lattice constants $a=b=4.126$ Å and $c=3.914$ Å. The antiferromagnetic exchange along the c axis chains is roughly 100 times stronger than the ferromagnetic exchange in the a-b plane. There is a small (0.2%) xy-like anisotropy in the exchange. The characteristic energy for 1D excitations is $\pi J=53$ meV. The system undergoes a phase transition to a 3D antiferromagnetic state at $T_N\approx 39$ K [26].

Neutron scattering measurements were carried out using the MARI chopper spectrometer on the ISIS pulsed neutron source. The sample was mounted in a closed cycle refrigerator so that its temperature could be controlled to within ± 0.1 K and aligned on a goniometer with the $(h,0,l)$ plane horizontal. A Fermi chopper was used to select a fixed incident neutron energy, E_0. In this Letter we limit our discussion to the results obtained with $E_0=148.9$ meV. The results for other values of E_0 are fully consistent with those reported here, and will be discussed in detail elsewhere [25].

MARI has low angle detectors 4 m from the sample arranged symmetrically in eight banks around the incident neutron axis. The range of scattering angle, ϕ, covered in the low angle banks extends 3.86° to 12°. Since the scattering in a quasi-1D material occurs in sheets in reciprocal space, if the crystal is aligned with the c axis parallel to the incident neutron wave vector, $\mathbf{k}_0$, the magnetic scattering at constant ϕ can be summed over all of the banks with no loss of information. This feature has been exploited to improve the statistics in our experiment.

When the time of flight method is used cross sections are measured along parabolic trajectories of ω and Q. There is a unique trajectory for each value of ϕ. Figure 1(a) shows the trajectory for $\phi=8°$ projected onto the chain direction for $E_0=148.9$ meV. The trajectory is plotted over an extended zone scheme showing ϵ_Q and ϵ_Q^u appropriate for $KCuF_3$. The intersection of the trajectory with the excitation continuum (shown by thick lines) corresponds to the expected region of inelastic magnetic scattering. Figure 1(b) shows the scattering observed in $KCuF_3$ at $T=20$ K with $\mathbf{c}\|\mathbf{k}_0$ and $E_0=148.9$ meV summed over all of the low angle detector banks. These data have been corrected for detector efficiencies and normalized to total detector solid angle and neutron monitor counts. A comparison with scattering from a vanadium standard was used to express the intensity in absolute units corresponding to mb/meV sr Cu, however, the overall conversion factor has a large uncertainty (approximately 30%).

The nonmagnetic background scattering was independently determined using the method we have developed previously [24] of measuring the scattering with $\mathbf{a}\|\mathbf{k}_0$. In this configuration the scattering in the vertical direction has no component of momentum transfer along the chain

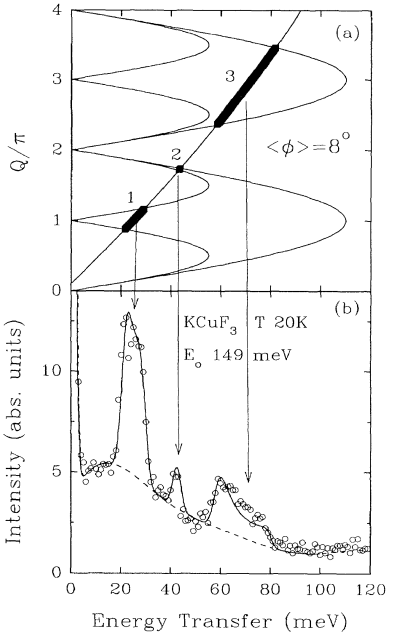

FIG. 1. (a) Scattering trajectory for $E_0=148.9$ meV and $\phi=8°$ for $\mathbf{k}_0$ along c^* in $KCuF_3$. Scattering results when the trajectory intersects with the continuum states (bold line). (b) Scattering actually observed in the MARI low angle banks at $T=20$ K. The nonmagnetic background is indicated by a dashed line. The solid line is a model fit as discussed in the text. The scattering is expressed in absolute units of mb/meV sr Cu atom.

direction, and the quasi-one-dimensional magnetic response is effectively zero. [Actually the nonzero width of each detector (30 cm) gives rise to a magnetic contribution, but we have found it to be small enough to be ignored.]

The solid line in Fig. 1(b) is the result of a fit using the nonmagnetic background plus the theoretical $T=0$ magnetic scattering. The latter has been calculated using the expression of M convolved with the instrumental resolution appropriate for a summation over all detectors. The nominal energy resolution of the spectrometer is roughly 1.5 meV (FWHM), but the summation over different scattering angles degrades the Q resolution and this is the dominant instrumental contribution. Near $Q=\pi$, a δ function mode with a dispersion relation given by ϵ_Q would lead to a sharp peak with an approximate FWHM of 4 meV on the plot of intensity versus energy transfer. The fitting parameters varied are an overall amplitude, the exchange constant, and a scaling factor multiplying the background. The background factor is necessary to correct for self-absorption, and leads to an adjustment of the order of 5% of the background intensity. The background is shown as a dashed line. The fitted value of the exchange energy, $\pi J=53$ meV, is to within experimental error equal to that obtained from earlier studies of the low energy scattering [21]. An excellent fit to the data is obtained over the entire spectrum. Since the thermal energies at 20 K are much lower than the energy transfer probed by the scattering, it is perhaps not too surprising that a $T=0$ calculation can describe the data. On the other hand, it is interesting to note that the 1D quantum effects are dominant well below the 3D ordering temperature.

Three domains of the spectrum are marked on the figure. Region 1 is the low energy scattering around $Q=\pi$, the antiferromagnetic point. The field theory calculations should apply in this region. Region 2 shows relatively sharp scattering from the branch close to the nuclear point. Region 3 contains high energy response extending well above the top of the dCP branch. The scattering cuts off very close to the theoretical upper bound ϵ_Q^u.

To investigate the Q dependence of the scattering the data can be further subdivided by scattering angle, substantially increasing the Q resolution. Figure 2 shows the scattering recorded at $T=20$ K in region 1 ($Q\approx\pi$) for concentric rings of scattering with the following values of ϕ: (a) 3.86°–6.43°, (b) 6.86°–8.14°, (c) 8.57°–9.86°, and (d) 10.29°–12°. The data have been normalized in the same way as the data of Fig. 1 and the nonmagnetic background subtracted. The extra resolution achieved by subdivision into rings is apparent. The solid lines are scattering profiles calculated for each ring at a temperature of 20 K using Eq. (4). The only adjustable parameter is an overall scaling factor which is identical for all rings. The calculation gives an excellent description of the scattering observed near $Q=\pi$, and, in particular,

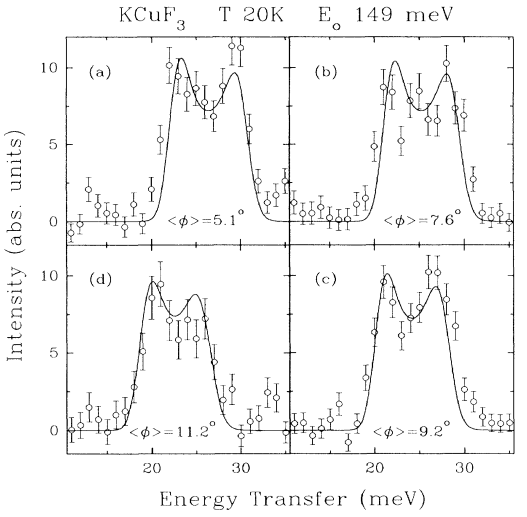

FIG. 2. Magnetic scattering with $\mathbf{k}_0$ along c^* observed at $T=20$ K for concentric rings of detectors corresponding to different scattering angles as discussed in the text. The weighted average scattering angle is indicated in each case. The calculated scattering is indicated by solid lines (see text).

reproduces the angular dependence completely. The position, line shape, and intensity of the magnetic scattering are accounted for very well. The double peaked structure reflects the fact that on either side of $Q=\pi$ the Q-ω trajectory of the scan intersects the region of strong scattering coinciding with ϵ_Q.

Figure 3 shows the temperature dependence of the scattering in region 1. To obtain adequate statistics at high temperatures the scattering has been summed over the low angle detector banks; the instrumental resolution is identical to that for the scan in Fig. 1(b). The data have been normalized and the background subtracted as in Fig. 2. The error bars represent 1 standard deviation determined from counting statistics only and do not reflect the additional uncertainty introduced by the subtraction of the nonmagnetic background. The temperatures shown range from 50 to 200 K, all above T_N. As expected, the scattering broadens and weakens as the temperature increases. The solid line is the calculated scattering using Eq. (4), with J and an overall amplitude fixed by the low temperature fits. The theoretical expression does not account for scattering arising from $Q\approx 2\pi$, which gives rise to the small peak around 42 meV. Aside from that, the agreement with experiment is outstanding over the entire temperature range. The small discrepancies between the theory and the data are within the systematic error in the background subtraction.

The spinon based theory provides an impressive account of the observed scattering. Conversely, classical theory for one-dimensional systems disagrees with the experiments. At zero temperature, a renormalized classical theory predicts sharp peaks at ϵ_Q, which would be

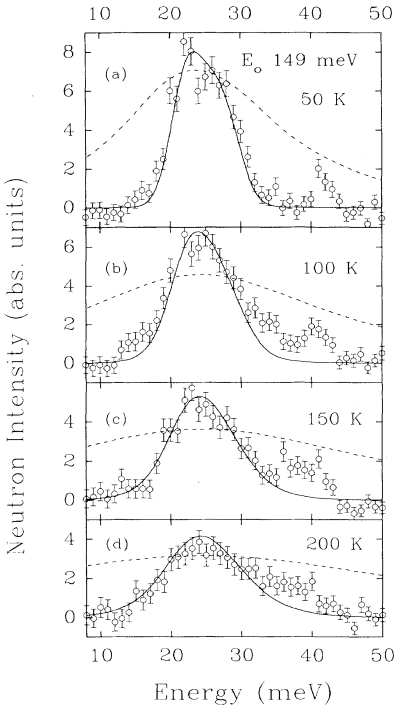

FIG. 3. Magnetic scattering in the MARI low angle detector bank with $\mathbf{k}_0$ along c^* at various temperatures: (a) 50 K, (b) 100 K, (c) 150 K, (d) 200 K. The solid lines represent the scattering predicted from a quantum field theory model as discussed in the text. The dashed lines show the scattering predicted from classical theory.

resolved easily with the resolution of the present experiment. This is incompatible with the broad continuum that is, in fact, observed. At higher temperatures the classical theory predicts that the mode broadens in a manner that can be described as a Lorentzian in energy centered at ϵ_Q with a Q independent FWHM equal to $4 \times k_B T$ [14]. This broadening is much greater than that predicted by the field theory calculation. This is illustrated by the dashed lines in Fig. 3, which show the classical prediction for the scattering, with the peak height normalized to fit on the same scale as the data.

In conclusion, we have carried out inelastic neutron scattering on the 1D magnet $KCuF_3$ as a function of temperature. The results are in quantitative agreement with a field theory calculation for $S^{aa}(Q,\omega)$. The scattering arises from unbound spinon pair excitations. Further experiments are called for to establish whether this is true for higher half-odd-integer spin values. A complete account of our current experiment, including a detailed discussion of the results for other values of E_0, is reported elsewhere [25].

The authors would like to acknowledge valuable discussions with A. M. Tsvelik, and the staff at RAL for their expert assistance, particularly Z. Bowden, A. D. Taylor, and M. Arai. This work has been supported by the U.S. DOE under Award No. DE-FG05-92ER45280, by the SERC, and by a NATO travel grant. The MARI chopper spectrometer is located at the ISIS pulsed neutron source of the Rutherford Appleton Laboratory, Oxon, United Kingdom, operated by the SERC.

[a]Permanent address: Rutherford Appleton Laboratory, Oxon, United Kingdom.

[1] See, e.g., J. C. Phillips, *Physics of High-T_c Superconductors* (Academic, San Diego, CA, 1989).
[2] R. B. Laughlin, Phys. Rev. Lett. **50**, 1395 (1983).
[3] F. D. M. Haldane, Phys. Rev. Lett. **50**, 1153 (1983); Phys. Lett. **93A**, 464 (1983).
[4] I. Affleck, J. Phys. Condens. Matter **1**, 3047 (1989).
[5] E. Fradkin, *Field Theories of Condensed Matter Systems* (Addison-Wesley, Redwood City, CA, 1991).
[6] P. W. Anderson, Mater. Res. Bull. **8**, 153 (1973).
[7] V. Kalmeyer and R. B. Laughlin, Phys. Rev. Lett. **59**, 2095 (1987).
[8] Z. Zou, Phys. Rev. B **40**, 2262 (1989).
[9] A. M. Tsvelik, Phys. Rev. B **45**, 486 (1992).
[10] P. W. Anderson, Phys. Rev. **86**, 694 (1952).
[11] P. W. Anderson, Science **235**, 1196 (1987).
[12] L. D. Faddeev and L. A. Takhtajan, Phys. Lett. **85A**, 375 (1981).
[13] See, for example, M. Steiner, J. Appl. Phys. **67**, 5593 (1990); J. P. Renard, J. Magn. Magn. Mater. **90**, 213 (1990), and references therein.
[14] H. H. Kretzen, H. J. Mikeska, and E. Patzak, Z. Phys. **271**, 269 (1974).
[15] H. J. Schulz, Phys. Rev. B **34**, 6372 (1986).
[16] H. A. Bethe, Z. Phys. **71**, 265 (1931).
[17] J. des Cloizeaux and J. J. Pearson, Phys. Rev. **128**, 2131 (1962).
[18] Y. Endoh, G. Shirane, R. J. Birgeneau, P. M. Richards, and S. L. Holt, Phys. Rev. Lett. **32**, 170 (1974).
[19] I. U. Heilmann, G. Shirane, Y. Endoh, R. J. Birgeneau, and S. L. Holt, Phys. Rev. B **18**, 3530 (1978).
[20] M. T. Hutchings, H. Ikeda, and J. M. Milne, J. Phys. C **12**, L739 (1979).
[21] S. K. Satija, J. D. Axe, G. Shirane, H. Yoshizawa, and K. Hirakawa, Phys. Rev. B **21**, 2001 (1980).
[22] G. Müller, H. Thomas, H. Beck, and J. C. Bonner, Phys. Rev. B **24**, 1429 (1981).
[23] A. Luther and I. Peschel, Phys. Rev. B **9**, 2911 (1974).
[24] S. E. Nagler, D. A. Tennant, R. A. Cowley, T. G. Perring, and S. K. Satija, Phys. Rev. B **44**, 12361 (1991).
[25] D. A. Tennant *et al.* (unpublished).
[26] M. T. Hutchings, E. J. Samuelsen, G. Shirane, and K. Hirakawa, Phys. Rev. **188**, 919 (1969).